Aust. J. Phys., 1984, **37**, 55–61

A Guide to the Determination of Operational Parameters in the Conventional X-ray Diffractometry of a Small Single Crystal

A. McL. Mathieson

Division of Chemical Physics, CSIRO,
P.O. Box 160, Clayton, Vic. 3168.

Abstract

There are two important operational parameters in conventional X-ray diffractometry of small crystals—scan range and detector aperture size. These parameters depend on a number of experimental factors, the main ones being the crystal mosaic spread μ, the source size σ and the wavelength distribution λ. Earlier theoretical analyses did not provide a procedure for establishing realistic estimates of these in an actual experimental set-up. Therefore, scan range and detector aperture size have been determined, not from the physical features of the experiment, but by *ad hoc* decisions, sometimes not far removed from 'guesstimates'. By considering the $(\Delta\omega, \Delta 2\theta)$ intensity distribution (Mathieson 1982) and by the selection of appropriate scan modes, it is possible to obtain experimental estimates of suitable outer limits of μ, σ and λ, namely a_μ, a_σ and b_λ, and hence to determine appropriate values of the scan range and aperture size for the reflections to be examined. From a comparison of an example using this method with previously published parameters, it is concluded that, in the majority of past cases of conventional analyses, the scan and aperture parameters chosen led (a) to a progressively decreasing $\Delta\lambda$ bandwidth as $\theta \to 90°$ and hence to erroneous determinations of temperature factors —a recognized defect—and (b) to a largely unrecognized defect, namely an overestimation of integrated intensity as $\theta \to 0°$, corresponding to a significant source of systematic error which could conceal the true extent of extinction.

1. Introduction

In the conventional, essentially one-dimensional, wide-aperture procedure of estimating integrated X-ray intensity from a small single crystal, once the scan mode has been selected, there are two operational parameters which require setting to ensure that the results for all reflections are placed on a comparable basis, at least within the limitations of this procedure (see Mathieson 1983*a*). These parameters are the specimen crystal scan range $\Delta\omega$ and the detector aperture size $\Delta 2\theta$.

Perusal of crystal structure analyses published over the last few years, for example, indicates a wide variation with respect to the magnitudes of these parameters, as well as to the relative weights of their wavelength-dependent and wavelength-independent components. In most cases, little explanation is offered for the values chosen. In some cases, in moving from one region of θ to another, the aperture size is adjusted when it should remain unchanged (see Mathieson 1983*b*) whereas, in other cases, it remains unchanged when it should properly be altered. Moreover, the decision as to the magnitude of the wavelength-dispersive component of these parameters, where relevant, does not always appear to be related to the physical features of the experiment.

0004-9506/84/010000$02.00

In the earlier literature (Furnas 1957; Alexander and Smith 1962, 1964*a*, 1964*b*; Burbank 1964, 1965; Ladell and Spielberg 1966; Kheiker 1969; Werner 1972; Einstein 1974; Denne 1977*a*), the situation was analysed largely in terms of a one-dimensional presentation of the reflection profile. Apart from the suggestions of Furnas (1957) and Alexander *et al.* (1963), it was not very clear from the theoretical studies how an experimentalist should proceed in a practical manner to derive physically reasonable parameters from an actual experimental set-up. As a result, in the case of most crystal structure studies, decisions concerning the parameters chosen can rarely stand up to critical examination.

Table 1. Scan range and detector aperture size for the main scan modes in terms of the components μ, σ, λ, c

Scan type	Scan range				Aperture size			
	μ	σ	λ	c	μ	σ	λ	c
ω	$a_\mu+a_\sigma+b_\lambda\tan\theta+a_c$					$a_\sigma+2b_\lambda\tan\theta+a_c\lvert\cos 2\theta+1\rvert$		
ω/θ	$a_\mu+a_\sigma+b_\lambda\tan\theta+a_c$				$\lvert-a_\mu\rvert$	$+\ b_\lambda\tan\theta+a_c\lvert\cos 2\theta\rvert$		
$\omega/2\theta$	$a_\mu+a_\sigma+b_\lambda\tan\theta+a_c$				$\lvert-2a_\mu\rvert+\lvert-a_\sigma\rvert$		$+a_c\lvert\cos 2\theta-1\rvert$	

2. The ($\Delta\omega, \Delta 2\theta$) Viewpoint

When one considers the problem on the basis of the two-dimensional ($\Delta\omega, \Delta 2\theta$) viewpoint given by Mathieson (1982), the situation is physically more comprehensible and the means of arriving at a decision as to the appropriate parameters becomes relatively straightforward. The relationships between the scan range and aperture size for the main types of scan are summarized in Table 1. The components μ, σ and λ represent the mosaic distribution of the crystal, the X-ray source emission distribution and its wavelength distribution respectively. The relative disposition of μ, σ and λ in ($\Delta\omega, \Delta 2\theta$) space can be represented in component diagrams for the different scan modes as in Fig. 1. The limits a_μ, a_σ and b_λ represent the ranges of the respective distributions in angular values of $\Delta\omega$ and their orientation relative to the axes of the diagrams. From the relations in ($\Delta\omega, \Delta 2\theta$) space indicated by Mathieson (1982, 1983*a*), the corresponding ranges in $\Delta 2\theta$ arising from the affine transformation associated with the specific scan can be deduced (see Mathieson 1983*c*). The contribution

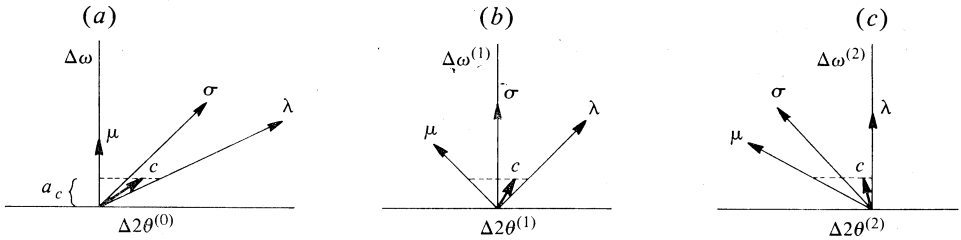

Fig. 1. The ($\Delta\omega, \Delta 2\theta^{(s)}$) component diagrams for (*a*) the ω scan mode ($s = 0$), (*b*) the ω/θ scan mode ($s = 1$) and (*c*) the $\omega/2\theta$ scan mode ($s = 2$). The affine transformation relating scan mode s to the ω scan mode is $\Delta\omega^{(s)} = \Delta\omega$ and $\Delta 2\theta^{(s)} = \Delta 2\theta^{(0)} - s\Delta\omega$. Here μ, σ and λ represent the three main components of crystal mosaicity, X-ray source distribution and wavelength distribution, while c represents the minor component, the (spherical) crystal dimension. The slope of the component in each diagram is related to the functional dependence for the particular scan mode.

due to the dimension of the crystal specimen c (Mathieson 1984), namely a_c, is included in Table 1. Generally it is much smaller than that of the source and will be ignored in what follows.

3. Procedure

With regard to the various a and b parameters, we consider first the wavelength-dispersive component $b_\lambda \tan\theta$. The decision concerning b_λ is a choice which is external to the equipment, being based on (i) the 'natural' spectral distribution of the radiation used, i.e. not convoluted with any other component of the experiment, and (ii) the wavelength range λ_1 to λ_2 elected by the experimentalist. Take, for example, the spectral distributions of two commonly used radiations Cu K_α and Mo K_α (Parratt 1936; Edwards and Langford 1971). From inspection of such spectral distributions, one can decide to set the limits λ_1 and λ_2 at points on the curve where the spectral intensity has fallen to (say) 1% of the peak (α_1) value. This will correspond to λ_1 being 3 (or 4) mÅ ($\equiv 10^{-13}$ m) less than λ_{α_1}, and λ_2 being 3 (or 4) mÅ more than λ_{α_2}. The separation of λ_{α_1} and λ_{α_2} is 4 mÅ so that the total $\Delta\lambda$ ($=\lambda_1-\lambda_2$) band will be 10 (or 12) mÅ. Since $b_\lambda = (180/\pi)(\Delta\lambda/\lambda)$, b_λ will be 0·37° or 0·45° for Cu K_α, and 0·81° or 0·97° for Mo K_α, depending on whether one chooses a 10 or 12 mÅ band.

The non-dispersive a components are, by contrast, internal determinants based on the main physical constituents of the experiment, μ and σ, and so a_μ and a_σ must be established by reference to measurements made on the actual apparatus concerned. For these estimates, it is preferable to operate with low-angle reflections (a) for the sake of intensity and (b) because the $b_\lambda \tan\theta$ contribution will be relatively small and any necessary correction minor. In the case of the $\omega/2\theta$ scan, this contribution in relation to the aperture is zero (see Table 1).

4. Experimental

The following example will indicate the possibilities of the $(\Delta\omega, \Delta 2\theta)$ method. The intensity distributions $I(\Delta\omega, \Delta 2\theta)$ are presented in contour form, the contour levels being on a logarithmic scale from the maximum to ~2% of the maximum. For convenience in presentation, only every second level of the original levels is drawn. The results were obtained using unfiltered Mo K_α radiation with a small crystal of K_2SnCl_6 of average dimension 0·1 mm. A Picker diffractometer was used with updated drives and computer control, but with its mechanical features essentially unchanged. The detector was a standard scintillation type with an aperture in front of dimension ~0·1 mm. In Fig. 2 the results are shown for the two reflections $1\bar{1}1$ at $\theta = 3{\cdot}5°$ and 404 at $\theta = 11{\cdot}5°$. Figs 2*a* and 2*c* correspond to $\omega/2\theta$ scans of the two reflections, while Fig. 2*b* corresponds to an ω/θ scan of $1\bar{1}1$. Peak counts per second were ~6000 for $1\bar{1}1$ and ~4000 for 404.

From Fig. 2*a*, it is evident that, for the conventional $\omega/2\theta$ scan procedure, an aperture of $\Delta 2\theta = 0{\cdot}30°$ would be appropriate. The result for the 404 reflection in Fig. 2*c* confirms this value which, as Table 1 shows, is applicable for the full range of θ. So we have $|-2a_\mu|+|-a_\sigma| = 0{\cdot}30°$. From Fig. 2*c*, one can also check the suitability of the value $b_\lambda = 1{\cdot}0°$, chosen for the wavelength-dispersive component. For this reflection, we have $\tan\theta = 0{\cdot}203$ so that $b_\lambda \tan\theta = 0{\cdot}20°$, this range, parallel to the $\Delta\omega$ axis, being indicated by the distance between the short lines L and L′. These lines coincide approximately with the 2% contour level in the region

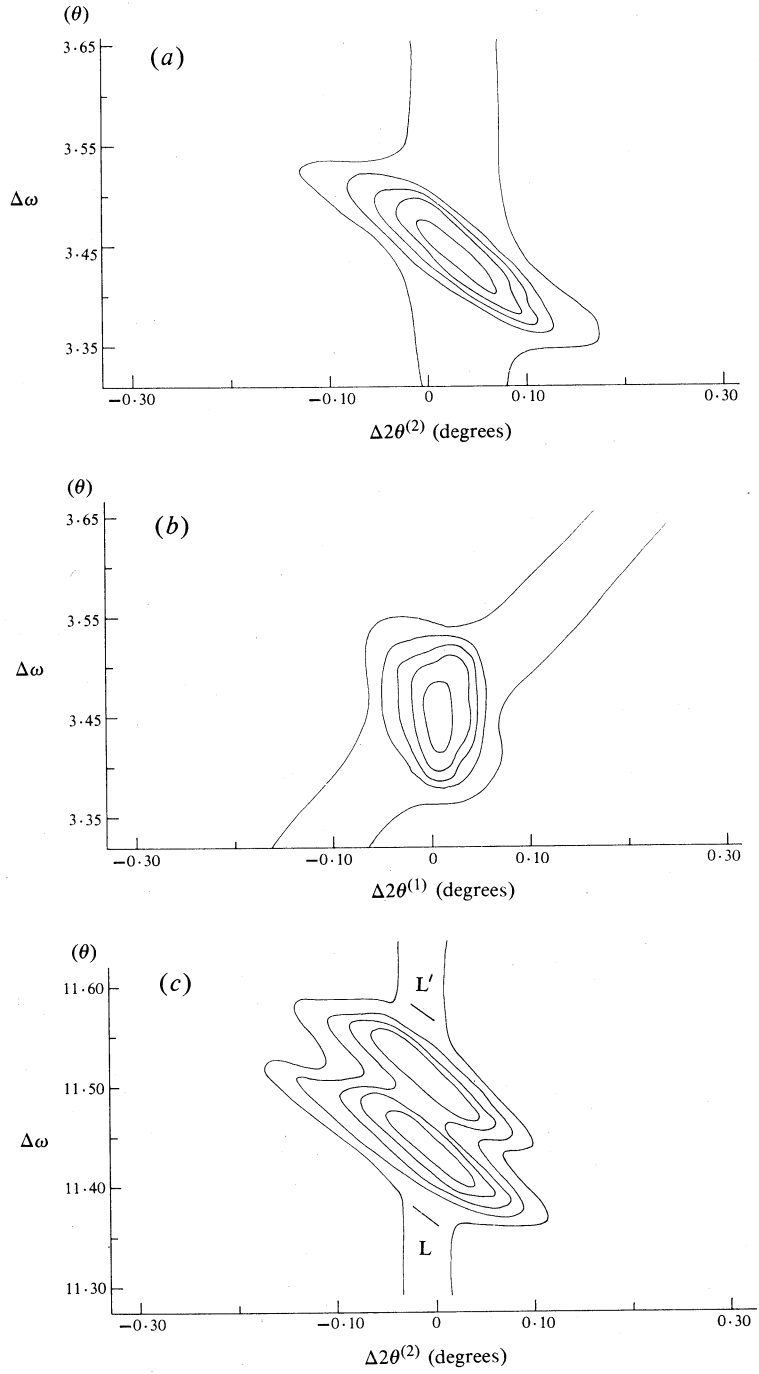

Fig. 2. Intensity distributions $I(\Delta\omega, \Delta 2\theta^{(s)})$ contoured on a logarithmic scale from the maximum intensity to ~2% of the maximum: (*a*) and (*b*) are for the $1\bar{1}1$ reflection and (*c*) for the 404 reflection of K_2SnCl_6. Parts (*a*) and (*c*) correspond to the $\omega/2\theta$ scan mode while (*b*) corresponds to the ω/θ scan mode. Peak counts per second were ~6000 for $1\bar{1}1$ and ~4000 for 404. In (*c*), the vertical distance between the short lines L and L′ represents $b_\lambda \tan\theta = 0{\cdot}20°$.

through the peaks and along the continuum (see Mathieson 1983*d*). It would appear ill-advised to use a value of b_λ significantly smaller than that chosen. Fig. 2*b* shows the result for an ω/θ scan of the $1\bar{1}1$ reflection. For this reflection and this scan mode, the minimum conventional aperture is a mere $0{\cdot}13°$. The $b_\lambda \tan\theta$ contribution is $0{\cdot}06°$ so that the estimate of a_μ is $0{\cdot}07°$. Together with the data from Figs 2*a* and 2*c*, this gives an estimate for a_σ of $0{\cdot}16°$. For the ω/θ scan mode, the appropriate aperture size $0{\cdot}07°+1{\cdot}0°\tan\theta$ would increase rapidly for higher θ angles. (With regard to Fig. 2*b*, it may be observed that, even at this low θ value, the existence of the α_2 component adjacent to the α_1 component, with separation $0{\cdot}02°$, is just visible. By the time that one reaches $\theta = 11{\cdot}5°$, the separation is $0{\cdot}06°$, and the resolution is excellent, see Fig. 2*c*.)

5. Discussion

One feature which will be noted by those who use diffractometers in the conventional way is the relatively small angular range associated with non-wavelength-dispersive components. When one surveys the magnitude of the two components A and B (of $A + B\tan\theta$), reported for the scan range in relation to published structure analyses with data collected in the conventional mode, the general pattern is $A > B$. By contrast, when one turns to the value of $B\,(=b_\lambda)$, derived here from a consideration of the 'natural' spectrum, and of $A\,(= a_\mu + a_\sigma + a_c)$, from typical estimates of mosaic spread and X-ray source size, the reverse tends to hold, namely $B > A$. The significance of these observations is that, in most structure analyses where the data collection has been based on the conventional procedure, the scan range (and aperture size) have been larger than advisable at low θ angles and smaller than advisable at high θ angles. The latter deviation from a proper measurement procedure produces the so-called truncation effect. This is a well-known effect (see e.g. Kheiker 1969), where the estimate of integrated intensity is less than it should be, where it becomes progressively worse as θ approaches 90°, and where it leads to erroneous (higher) estimates of temperature factors (see e.g. Denne 1977*b*). The former deviation, of A being larger than necessary, has gone essentially unnoticed. The consequence is that integrated intensity estimates in the low θ region are larger than they should be, the difference being greater the lower the θ angle. This therefore constitutes a systematic source of error which could conceal the full extent of extinction. Because of its impact in the low θ region, its effect is potentially significant for bonding electron density studies.

The procedure discussed here for establishing proper estimates of scan range and aperture size should assist in ensuring that the error sources referred to above are minimized where the conventional mode of operation is used. As Mathieson (1982) has noted earlier, the problem is not truncation itself, but variable truncation.

Since the size of the wavelength-dispersive factor $b_\lambda\ (=B)$ proposed here is considerably larger than those derived from earlier suggestions, it is perhaps advisable to refer to this matter in more detail. Earlier workers proposed that the estimate of B should be based on the separation of the α_1 and α_2 components plus contributions based on the 'natural' widths of the α_1 and α_2 components, scaled by an arbitrary factor k (see Burbank 1964; p. 436). Numerical estimates derived for Cu and Mo radiation on the basis of these proposals are given in Table 2 and compared with the approach taken in this paper. The present results give values for b_λ higher by 150–200%. As Burbank has commented, the limits selected to truncate the λ distri-

bution are, in a sense, arbitrary. However, in practice, they should be chosen so that small displacements of the total $\Delta\lambda$ band are not critical, i.e. they occur where the slopes of the distribution at the outer limits of the band are small and opposite in sign. Hence, the choice is given here at 1% of the peak level. It may also be noted that, on the basis of the width at half-height, the interval λ_{α_2} to λ_2 is generally larger than the interval λ_1 to λ_{α_1} (see Table 2). Taking into account that the intensity of the α_2 peak is about half that of the α_1 peak, nomination of $\lambda_1-\lambda_{\alpha_1}$ and $\lambda_{\alpha_2}-\lambda_2$ as equal is a simple and workable solution.

Table 2. Various estimates of the wavelength dispersion component b_λ ($=B$)

Here k is the factor for multiplying the 'natural' widths of α_1 and α_2 (see Parratt 1936). The wavelength units are mÅ, and b_λ is in degrees. The separation of α_1 and α_2 is taken to be 4 mÅ

Source[A]	k	Mo				Cu			
		$\lambda_1-\lambda_{\alpha_1}$	$\lambda_{\alpha_2}-\lambda_2$	$\lambda_1-\lambda_2$	b_λ	$\lambda_1-\lambda_{\alpha_1}$	$\lambda_{\alpha_2}-\lambda_2$	$\lambda_1-\lambda_2$	b_λ
Furnas	1·0	0·268	0·280	4·55	0·37	0·460	0·635	5·10	0·19
Alexander & Smith	2·5	0·67	0·70	5·37	0·43	1·15	1·588	6·59	0·24
Burbank	3·15	0·84	0·88	5·72	0·46	1·449	2·0	7·45	0·28
Present work	—	4·0	4·0	12·0	0·97	4·0	4·0	12·0	0·45
		(3·0)	(3·0)	(10·0)	(0·81)	(3·0)	(3·0)	(10·0)	(0·37)

[A] See Burbank (1964; p. 436).

The observations made here stress once again that, when an ω or ω/θ scan is being used, variation in the aperture size is obligatory with a change in θ. For this, an aperture which opens symmetrically will be adequate.

The presentation in this paper is intended to assist in making best use of the conventional diffractometer procedure for the collection of intensity data. It does not permit one to make allowances for the extraneous contributions inherent in the classical procedure (see Mathieson 1982). These can be excluded with the boundary-following asymmetric aperture procedure (Mathieson 1983*a*).

Acknowledgments

I am grateful to W. Fock for his computer programs to provide contour maps of the intensity distributions and to interconvert the display for one scan mode to that for another, and also to S. L. Mair for use of data from K_2SnCl_6 and for a critical and helpful reading of the text.

References

Alexander, L. E., and Smith, G. S. (1962). *Acta Crystallogr.* **15**, 983–1004.
Alexander, L. E., and Smith, G. S. (1964*a*). *Acta Crystallogr.* **17**, 447–8.
Alexander, L. E., and Smith, G. S. (1964*b*). *Acta Crystallogr.* **17**, 1195–1201.
Alexander, L. E., Smith, G. S., and Brown, P. E. (1963). *Acta Crystallogr.* **16**, 773–6.
Burbank, R. D. (1964). *Acta Crystallogr.* **17**, 434–42.
Burbank, R. D. (1965). *Acta Crystallogr.* **18**, 88–97.
Denne, W. A. (1977*a*). *Acta Crystallogr.* A **33**, 438–40.
Denne, W. A. (1977*b*). *Acta Crystallogr.* A **33**, 987–92.
Edwards, H. J., and Langford, J. I. (1971). *J. Appl. Crystallogr.* **4**, 43–50.
Einstein, J. R. (1974). *J. Appl. Crystallogr.* **7**, 331–44.
Furnas, T. C. (1957). 'Single Crystal Orienter Instruction Manual' (General Electric Company: Milwaukee).

Kheiker, D. M. (1969). *Acta Crystallogr.* A **25**, 82–7.
Ladell, J., and Spielberg, N. (1966). *Acta Crystallogr.* **21**, 103–18.
Mathieson, A. McL. (1982). *Acta Crystallogr.* A **38**, 378–87.
Mathieson, A. McL. (1983*a*). *Aust. J. Phys.* **36**, 79–83.
Mathieson, A. McL. (1983*b*). *J. Appl. Crystallogr.* **16**, 572–3.
Mathieson, A. McL. (1983*c*). *J. Appl. Crystallogr.* **16**, 257–8.
Mathieson, A. McL. (1983*d*). *Acta Crystallogr.* A **39**, 79–83.
Mathieson, A. McL. (1984). The minimum scan range and detector aperture as a function of specimen size in X-ray diffractometry. *J. Appl. Crystallogr.* **17** (in press).
Parratt, L. G. (1936). *Phys. Rev.* **50**, 1–15.
Werner, S. A. (1972). *Acta Crystallogr.* A **28**, 143–51.

Manuscript received 8 July, accepted 19 September 1983